

H_I in Arp72 and similarities with M51-type systems

Chandreyee Sengupta,^{1*} D.J. Saikia² and K. S. Dwarakanath³

¹ *Calar Alto Observatory, IAA-CSIC, Spain*

² *National Centre for Radio Astrophysics, Tata Institute of Fundamental Research, Pune 411 007, India*

³ *Raman Research Institute, Bangalore 560 080, India*

ABSTRACT

We present neutral hydrogen (H_I) observations with the Giant Metrewave Radio Telescope (*GMRT*) of the interacting galaxies NGC5996 and NGC5994, which make up the Arp72 system. Arp72 is an M51-type system and shows a complex distribution of H_I tails and a bridge due to tidal interactions. H_I column densities ranging from $0.8\text{--}1.8 \times 10^{20}$ atoms cm⁻² in the eastern tidal tail to $1.7\text{--}2 \times 10^{21}$ atoms cm⁻² in the bridge connecting the two galaxies, are seen to be associated with star-forming regions. We discuss the morphological and kinematic similarities of Arp72 with M51, the archetypal example of the M51-type systems, and Arp86, another M51-type system studied with the *GMRT*, and suggest that a multiple passage model of Salo & Laurikainen may be preferred over the classical single passage model of Toomre & Toomre, to reproduce the H_I features in Arp72 as well as in other M-51 systems depicting similar optical and H_I features.

Key words: galaxies: spiral - galaxies: interactions - galaxies: kinematics and dynamics - galaxies:individual: Arp72, Arp86, M51 - radio lines: galaxies - radio continuum: galaxies

1 INTRODUCTION

The role of tidal interactions, collisions and mergers of galaxies in driving and shaping galaxy evolution over cosmic time scales, often triggering bursts of star formation, has been widely recognized since the early work by Toomre & Toomre (1972) as well as from many recent pieces of work (see Kennicutt, Schweizer & Barnes 1998; Barnes & Hernquist 1992; Barnes 1999; Struck 1999; Schweizer 2000, 2005). However, studies of gravitational interactions at optical wavelengths have often focussed on major mergers which involve galaxies of similar mass, leading to spectacular structures. Minor mergers with mass ratios in the range of $\sim 0.1\text{--}0.5$ may appear less spectacular at optical wavelengths, but show clear and complex signs of interactions in their H_I distributions as seen for example in M51 (Rots et al. 1990) and Arp86 (Sengupta, Dwarakanath & Saikia 2009). Although such minor mergers and interactions have so far usually been studied in the nearby Universe, more sensitive H_I observations with present and upcoming telescopes should enable us to examine such interactions at higher redshifts and add to our knowledge of galaxy growth and evolution through minor mergers and interactions. An important parameter to quantitatively assess the importance of interactions and mergers is the merger rate, which is the number of mergers per unit time and unit co-moving volume, which appears to increase with redshift (e.g. Abraham et al. 1996; Ryan et al. 2008). Identification, imaging and modelling of a large number of M51-type systems will

give us a better idea of the range of merger time-scales and hence the merger rate for these minor mergers and interactions.

In addition to mergers and interactions, there has also been a lot of interest in understanding how star formation rates are affected by collisions and mergers of galaxies since the early pioneering pieces of work by Larson & Tinsley (1978) and Struck-Marcell & Tinsley (1978). Observations with the Infrared Astronomy Satellite (*IRAS*) drew attention to the highly luminous infrared galaxies, the more extreme ones with far infrared luminosities greater than $10^{12}L_{\odot}$ being christened as ultraluminous infrared galaxies (Sanders et al. 1988). These are believed to be the result of mergers of similar-mass, gas-rich galaxies (see Soifer et al. 1987; Smith et al. 1987; Sanders & Mirabel 1996; Struck 1999). The high resolution of *Spitzer* infrared observations have made it possible to study individual star-forming regions (see Smith et al. 2007, and references therein). The advent of the Galaxy Evolution Explorer (*GALEX*) ultraviolet (UV) telescope, has provided another window to study stellar populations and star-formation history in galaxies (see Smith et al. 2010, and references therein). Ultraviolet observations show that tidal features are often quite bright at these wavelengths (e.g. Neff et al. 2005; Hancock et al. 2007), and are sometimes also known to reveal new tidal features, as seen in the interacting galaxy NGC4438 in the Virgo cluster (e.g. Hummel & Saikia 1991; Hota, Saikia & Irwin 2007) by Boselli et al. (2005). At radio frequencies, both H_I and CO observations have been good tracers of gas distributions for understanding the star-formation process (e.g. Helfer et al. 2003; Greve et al. 2005; Leroy et al. 2008, 2009; Walter et al. 2008; Bigiel et al. 2008), while continuum observations have been useful to constrain star-formation and supernova

* e-mail: sengupta@ncra.tifr.res.in(CS)
dwaraka@rri.res.in(KSD)

djs@ncra.tifr.res.in(DJS),

Table 1. GMRT observations

Frequency	Observation date	Phase calibrator	Phase cal flux density (Jy)	τ (hr)	Bandwidth (MHz)	rms (per channel for 21-cm line) (mJy beam ⁻¹)	Beam size		
							maj (")	min (")	PA (°)
21-cm line	2008 Apr 30	J1609+266	5.0	7	8	0.5	9.0	9.0	
						0.9	29.0	21.0	119
						1.0	41.0	35.0	126
1403 MHz						0.17	3.5	2.2	40

rates (see Condon 1992 for a review), as well as probe deep into the circumnuclear regions to study the supernova remnants and HII regions, as in the archetypal starburst galaxies M82 (Fenech et al. 2008, and references therein) and NGC1808 (Saikia et al. 1990; Collison et al. 1994).

In this paper, we present the results of H I observations of the interacting galaxies in Arp 72, which were observed as part of an ongoing H I survey of interacting galaxies to study their H I properties and the correlation of gas and stars in these galaxy pairs. Arp72 is an M51-type system, and such systems have often been used as laboratories for understanding the possible dynamics that give rise to the striking spiral arms, and tidal bridges and tails, as well as the correlation of gas and stars in these features (Salo & Laurikainen 1993, 2000; Reshetnikov & Klimanov 2003). We also present a comparative analysis of our results on the two M51-type systems we have studied so far, Arp72 and Arp86, with M51. The results for Arp86 were presented earlier by Sengupta, Dwarakanath & Saikia (2009). For comparison with M51, we have used the results from The H I Nearby Galaxy Survey (THINGS; Walter et al. 2008).

2 ARP72

Arp72 is a nearby unequal-mass interacting galaxy pair undergoing an intense phase of star formation. The system consists of NGC5996, the bigger galaxy of morphological classification SBc, at a radial velocity of 3297 ± 2 km s⁻¹, and the smaller companion NGC5994, a possible barred spiral, at a radial velocity of 3290 ± 10 km s⁻¹. The angular diameters of NGC5996 and NGC5994 are $\sim 1.6'$ and $0.6'$ respectively, which translates to a physical extent of ~ 20 and 8 kpc respectively, at a distance of 43.9 Mpc to the system (1 arcsec = 0.21 kpc). Throughout this paper, 43.9 Mpc has been used as the distance to the system, which has been estimated using their average optical velocity and a Hubble constant of 75 km s⁻¹ Mpc⁻¹. The morphological classifications, angular diameters and the optical radial velocities are from the NASA/IPAC Extragalactic Database (NED). NGC5996, is known to be a Markarian galaxy (Mrk691), with enhanced star formation possibly initiated by the interaction with NGC5994. The system has been a part of several statistical studies (Kandalyan 2003; Schwartz et al. 2006; Woods, Geller & Barton 2006), but has not been studied systematically at radio frequencies. Recently Smith et al. (2010) have presented a *GALEX* image of the system which shows a long ‘beaded’ tail towards the east of the main galaxy, which although seen in the Sloan Digital Sky Survey (SDSS) and Arp Atlas images, is more pronounced at UV wavelengths. The bridge connecting the two galaxies is also bright in the *GALEX* image. The bridge and the northern spiral arm are quite bright in H α (Smith et al. 2010), and the oxygen abundance in the centre of the bridge, $\log[\text{O}/\text{H}] + 12$, is ~ 8.7 (Hancock et al. in preparation; Smith et al. 2010).

3 OBSERVATIONS

Arp72 was observed for 7 hours in H I 21-cm line on 2008 April 30, using the Giant Metrewave Radio Telescope (*GMRT*). The full width at half maximum of the primary beam of *GMRT* antennas is $\sim 24'$ at 1420 MHz. The baseband bandwidth used was 8 MHz for the 21-cm H I line observations giving a velocity resolution of ~ 13.7 km s⁻¹. Some of the parameters of the observations and also the rms noise and beam sizes for the results presented here are summarized in Table 1.

Data obtained with the *GMRT* were reduced using AIPS (Astronomical Image Processing System). Bad data due to dead antennas and those with significantly lower gain than others, and radio frequency interference (RFI) were flagged and the data were calibrated for amplitude and phase using the primary and secondary calibrators. The primary flux density calibrator was 3C286, while the phase calibrator was J1609+266 (see Table 1). The flux densities are on the scale of Baars et al. (1977) and the error on the flux density is ~ 5 per cent. The calibrated data were used to make both the H I line images and the 1403-MHz radio continuum images by averaging the line-free channels and self calibrating. For the H I line images the calibrated data were continuum subtracted using the AIPS tasks ‘UVSUB’ and ‘UVLIN’. The task ‘IMAGR’ was then used to get the final 3-dimensional deconvolved H I data cubes. From these cubes the total H I images and the H I velocity fields were extracted using the AIPS task ‘MOMNT’. To examine the structures on different levels in both H I and radio continuum, we produced images of different resolutions by tapering the data to different uv limits.

4 OBSERVATIONAL RESULTS

4.1 H I morphology of Arp72

The low-resolution H I column density image of Arp72, with an angular resolution of $\sim 40''$ which corresponds to a linear resolution of ~ 8.5 kpc, overlaid on the optical r-band SDSS image is shown in the upper panel of Fig. 1. The corresponding H I spectrum of the system is shown in the lower panel of Fig. 1. The integrated flux density estimated from this spectrum is 30.1 Jy km s⁻¹ and the corresponding H I mass is $1.4 \times 10^{10} M_{\odot}$, for a distance of 43.9 Mpc to the system. Our total flux density is somewhat higher than the value of 22.97 ± 0.34 Jy km s⁻¹ estimated by Giovanardi & Salpeter (1985) from an Arecibo spectrum of the galaxy pair (UGC10033) over a size of 3.8×2.8 arcmin², and the HIPASS (H I Parkes All Sky Survey; Barnes et al. 2001) estimate of ~ 19.7 Jy km s⁻¹ (Wong et al. 2009). The lower flux densities for the Arecibo and HIPASS observations are likely to be due to the higher rms noise values of these observations, which are ~ 3 and 10 times higher than that of the *GMRT* observations. To explore this possibility, we convolved the low-resolution *GMRT* cube ($\sim 40''$) to be of similar res-

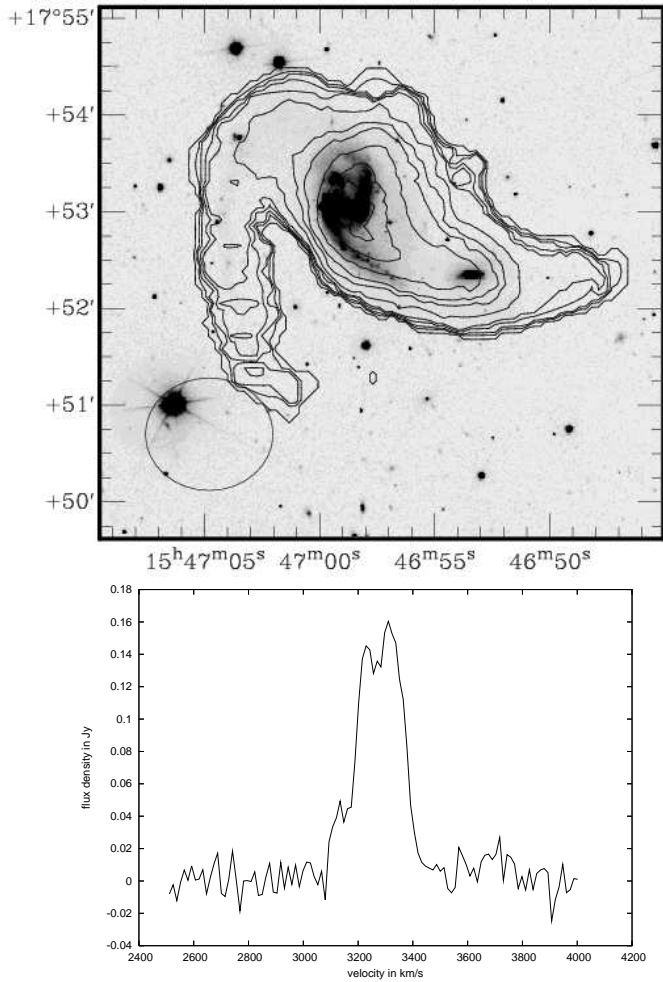


Figure 1. Upper panel: H_I column density contours obtained from the low-resolution (~ 40 arcsec) map, overlaid on the optical r-band SDSS image. The H_I column density levels are $1.14 \times (3, 7, 10, 15, 20, 35, 55, 70, 100, 130, 150, 170) \times 10^{19}$ atoms cm^{-2} . Beam plotted at bottom left. Lower panel: H_I spectrum of the Arp72 system obtained from the low-resolution data cube.

olution to the Arecibo beam (~ 3 arcmin) and estimated the flux density using a threshold similar to the rms noise of the Arecibo survey of ~ 3 mJy. The integrated flux density decreased from our estimate of $30.1 \text{ Jy km s}^{-1}$ to $20.3 \text{ Jy km s}^{-1}$, indicating that higher rms noise values for observations of this source with extended diffuse emission could lead to lower estimates of the integrated flux density.

Extended tidal tails and debris, expected from the interaction between NGC5996 and NGC5994, are seen around the system. An H_I bridge, aligned to the optical and UV ones which connects NGC5996 to its low-mass companion, is clearly seen. In addition, there is a long (~ 3.8 arcmin, ~ 50 kpc) tidal tail that originates at the northern edge of the disk of the larger galaxy NGC5996, curves towards the east and then towards the south, while the smaller galaxy NGC5994 exhibits an H_I extension towards the west. These features are reminiscent of those seen in M51 (Rots et al. 1990) and Arp86 (Sengupta et al. 2009). The corresponding velocity field is shown in Fig. 2. The disk of NGC5996 shows regular rotation; however, signatures of tidal interaction with NGC5994 are seen at the edge of the disk in the form of disturbance in that regular rotation pattern.

A moderate-resolution (~ 25 arcsec which corresponds to ~ 5.3

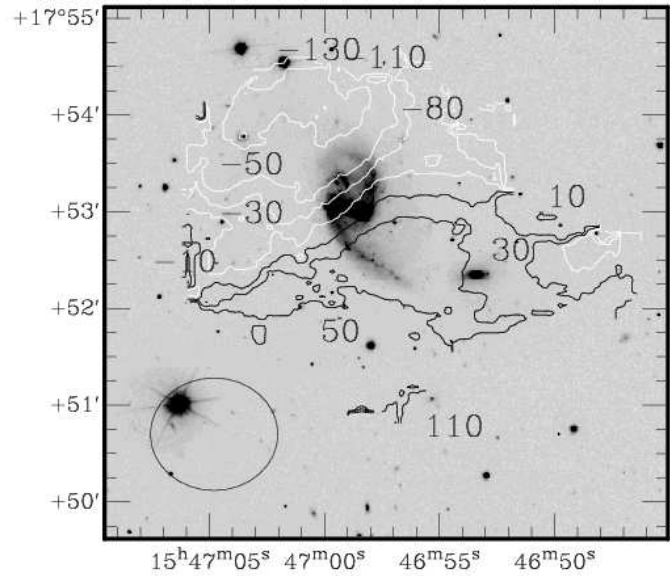


Figure 2. Radial velocity subtracted H_I velocity field at low resolution (~ 40 arcsec) overlaid on the r-band SDSS optical image. The velocities plotted are $-130, -110, -80, -50, -30, -10, 10, 30, 60, 110 \text{ km s}^{-1}$. The negative velocities are in white and the positive velocities are in black contours. Beam plotted at bottom left.

kpc) image of the Arp72 system is presented in Fig. 3 overlaid on the far-ultraviolet *GALEX* image, which has an effective bandpass of $1350\text{--}1705 \text{ \AA}$. The main features are similar to those seen in the low-resolution map, although the ridge of high H_I surface brightness is better defined, and the eastern tail seen in the *GALEX* image lies along the ridge line of the eastern H_I tail. In the high-resolution image, which has a resolution of ~ 10 arcsec, which corresponds to ~ 2 kpc, only the high H_I column density regions are seen. Overlays of the high-resolution H_I image of Arp72 system on the *Spitzer* 24-micron image, as well as on the *GALEX* UV image are shown in Fig. 4. The 24-micron image reveals the relatively new star forming zones and H_I is seen to be well correlated with the bright regions in the *Spitzer* image. The central star-forming region of the galaxy NGC5996 is devoid of H_I, which is often seen in many star-forming galaxies, possibly due to a combination of the gas being in molecular form as well as ionization of the H_I gas by the hot, young stars. The remaining parts of the main disk, including the northern spiral arm, as well as the tidal bridge between the two galaxies show the presence of dense H_I clumps with column densities as high as $\sim 2 \times 10^{21} \text{ atoms cm}^{-2}$.

4.2 Radio continuum emission

The radio continuum image at 1403 MHz with a resolution of ~ 3 arcsec (~ 0.6 kpc) obtained from the *GMRT* data, is shown in Fig. 5. The *GMRT* and FIRST (Faint Images of the Radio Sky at Twenty Centimeters; Becker, White & Helfand 1995) images are very similar, which show a compact radio source associated with the nuclear region of NGC5996, along with more diffuse emission, similar to the high-resolution structure seen in many spiral galaxies (e.g. Saikia et al. 1994). No emission has been detected from the smaller companion NGC5994. The NRAO VLA Sky Survey (NVSS; Condon et al. 1998) image also shows no emission from NGC5994, but shows an extended tail of emission along a PA of $\sim 22^\circ$, which extends from NGC5996 well beyond the bridge of emission con-

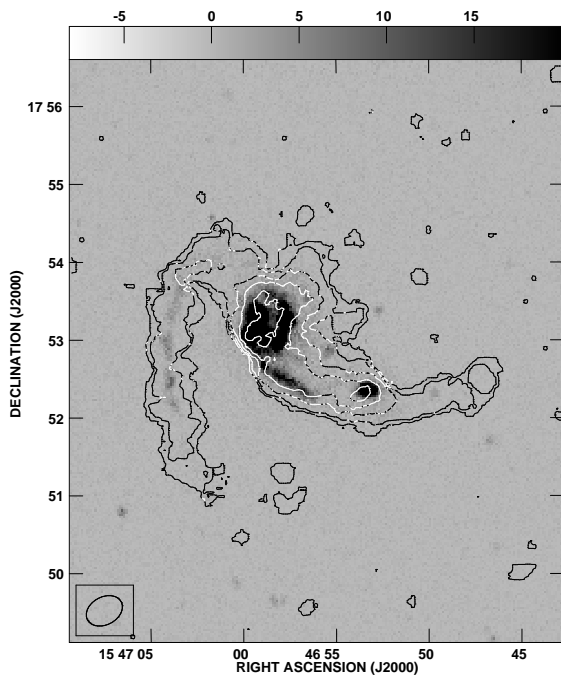


Figure 3. H I column density contours obtained from the medium resolution (~ 25 arcsec) map, overlaid on the *GALEX* image. The H I column density levels are $2.6 \times (3, 7, 15, 25, 40, 60) \times 10^{19}$ atoms cm^{-2} .

necting the two galaxies. Possible confusion from a background source cannot be ruled out. The total flux density of NGC5996 estimated from the *GMRT* image is ~ 22 mJy, while the peak and total flux densities, estimated from the NVSS image, including emission from the tail, are 20.4 mJy beam^{-1} and ~ 35 mJy respectively. NED lists the continuum flux densities of NGC5996 as 29.6 , 32 ± 4 and < 30 mJy at 1400 , 2380 and 5000 MHz respectively, taking the values from Condon, Cotton & Broderick (2002), Dressel & Condon (1978) and Kojan et al. (1980) respectively. Although these values suggest a rather flat radio spectrum at cm wavelengths, suggesting that thermal free-free emission as well as absorption by dense gas could be playing a significant role, the spectrum needs to be determined reliably using measurements at a larger number of frequencies. NGC5996 has been classified as a starburst, and it would be useful to determine its structure with sub-arcsec resolution to identify any possible AGN. It is relevant to note that the dominant galaxy in the Arp86 system, NGC7753, which has a high star-formation rate of $\sim 9 M_{\odot} \text{ yr}^{-1}$, exhibits a flat radio spectrum with $\alpha \sim 0.25$ ($S \propto \nu^{-\alpha}$) between 606 and 1394 MHz (Sengupta et al. 2009). In the case of M51, although the integrated spectrum is steep between 1415 and 2280 MHz with $\alpha \sim 0.87 \pm 0.04$, the spectrum of the nuclear region is relatively flat with $\alpha \sim 0.68 \pm 0.01$ (Klein, Wielebinski & Beck 1984). Studies of the central region of M51 show evidence of intense star formation possibly triggered by the interaction. For example, in the circumnuclear region, Nikola et al. (2001) use PDR models to estimate that the far-ultraviolet field intensities are similar to those found near OB star-forming molecular clouds in the Milky Way, a few hundred times the local Galactic interstellar radiation field.

5 DISCUSSION

Sensitive H I observations (column density $\leq 10^{20}$ atoms cm^{-2}) of nearby galaxies reveal details which could be related to the galaxy formation and evolution processes. In addition, to get a comprehensive picture of aspects such as the kinematics of the outer disks and warps, star formation law at low H I column densities, accretion of gas and signatures of dwarf companions around the galaxies, deep H I imaging of the systems are necessary. In this Section, we discuss our results on Arp 72, the M51-type system in our sample.

5.1 H I and star formation in the Arp72 system.

The star-formation rate (SFR) in the disks of spirals and starburst galaxies commonly follows the relation $\Sigma_{\text{SFR}} \propto \Sigma_{\text{gas}}^N$ with $N \sim 1.4$, and is often referred to as the Schmidt law (Schmidt 1959; Kennicutt 1989). The most recent and extensive study of the SFR and star-formation thresholds in nearby galaxies has perhaps come from the THINGS survey (Leroy et al. 2008; Bigiel et al. 2008). Bigiel et al. (2008) find that a molecular Schmidt law with an index $N = 1.0 \pm 0.2$ relates Σ_{H_2} to Σ_{SFR} in their sample of spirals. Bigiel et al. (2008) do not observe a universal relationship between total gas surface density and Σ_{SFR} with variations both within and amongst galaxies. In some cases they find a wide range of SFRs with very similar gas densities, while others seem to follow the Schmidt law over several orders of magnitude in gas surface density. They find the value of N to vary over a wide range from 1.1 to 2.7 , suggesting that there might not be a universal Schmidt law. They also suggest a link between the environment and relationships between gas and star formation, and star formation is not merely a function of gas surface density but also the physical conditions that set the ratio of H I to H_2 . Earlier observations also showed evidence of star formation happening in a wide range of densities and environments. For example, the H I bridge in the Magellanic Clouds, which has typical column densities $\sim 10^{20} - 10^{21}$ atoms cm^{-2} is known to have star formation occurring in it (Harris 2007), and no intense star formation is seen in the more diffuse Magellanic stream with $N(\text{H I}) \leq 3 - 5 \times 10^{20}$ atoms cm^{-2} (Bruns et al. 2005). However, H II regions have been found in tidal debris which are free of any significant H I association (Ryan-Weber et al. 2004).

Our observations of Arp72 also seem to confirm the above findings that there might not be a universal Schmidt law. Arp72 is undergoing a stage of intense star formation, possibly triggered by the interaction. NGC5996 has been classified by Balzano (1983) to have a starburst galactic nucleus, and it also shows evidence of star formation in the disk and spiral arms. The 24-micron band of *Spitzer* seems to be well suited for tracing recent star formation (Calzetti et al. 2005, 2007). Calzetti et al. (2005) reported a tight correlation between $\text{Pa}\alpha$ and 24-micron flux density in their study of star formation in NGC 5194 (M51a). The $\text{H}\alpha$ and UV emission have been used traditionally for studying star-formation, but both could be significantly affected by dust attenuation, although $\text{H}\alpha$ to a much smaller degree than UV. Compared with, say $\text{H}\alpha$ which traces early to mid-O type stars with ages less than about 10 Myr, the UV traces somewhat older and less massive stars of O to early-B type with ages of less than ~ 400 Myr, providing a star-formation measure over a longer time scale (see Calzetti et al. 2007; Smith et al. 2010).

To investigate the SF region to H I column density relation in this system, high resolution H I images were overlaid on the *GALEX* FUV and *Spitzer* 24-micron images and compared. A range of H I column densities from low to high are seen to be associated with

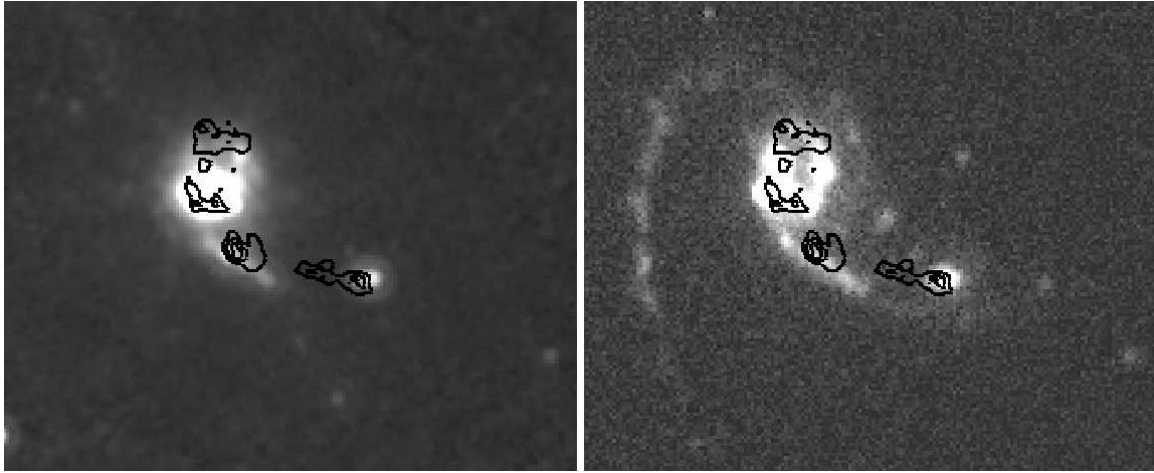


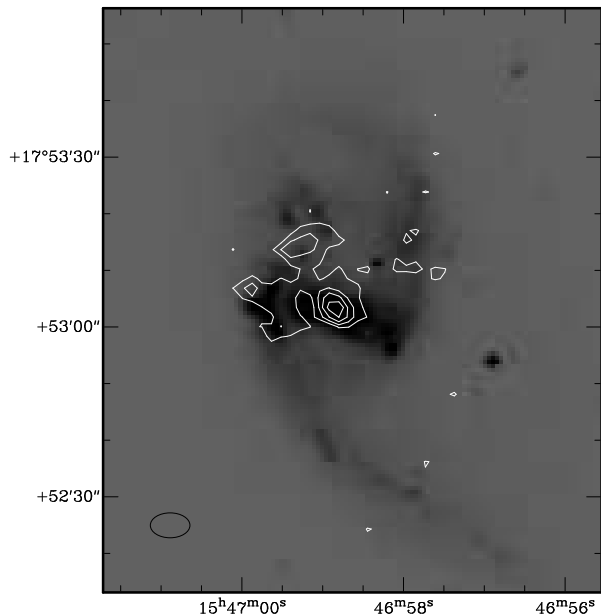
Figure 4. H I column density contours obtained from the high-resolution (~ 10 arcsec) map, overlaid on the *Spitzer* 24-micron (left panel) and *GALEX* far-ultraviolet (right panel) images. The H I column density levels are $(1.7, 2.1) \times 10^{21}$ atoms cm^{-2} .

the star forming regions. The high-resolution H I image with an angular resolution of ~ 10 arcsec (~ 2 kpc) shows H I clumps with column densities as high as $\sim 2 \times 10^{21}$ atoms cm^{-2} close to the 24-micron peaks of emission in the bridge (Fig. 4). Similar features are seen in the vicinity of the companion galaxy NGC5994, and from the disk and towards the north of the main galaxy NGC5996. A prominent tidal tail of H I seen towards the east of NGC5996 in the moderate- and low-resolution images is not visible in the high-resolution H I one (Figs. 3 and 4). This tail towards the east is barely visible in the *Spitzer* and SDSS images, but is very clearly seen in the *GALEX* image at UV wavelengths. The H I column densities estimated in the eastern tail are in the range of 0.8 to 1.8×10^{20} atoms cm^{-2} , and overlaps with the star-forming region seen most clearly in the *GALEX* image. Inspection of this system does not reveal any prominent star forming region associated with low ($< 10^{20}$ atoms cm^{-2}) H I column densities.

Using the empirical formula from Calzetti et al. (2007) and the 24-micron *Spitzer* flux densities from Smith et al. (2007), the SFR in NGC5996, NGC5994 and the tidal bridge were estimated to be 1.43, 0.06 and 0.21 $M_{\odot} \text{ yr}^{-1}$ respectively. NGC5994 is relatively quiescent compared to NGC5996. The high-resolution *GMRT* continuum image shows a compact component in the centre of NGC5996, and more diffuse emission towards the east and the north, while no radio continuum emission has been detected from NGC5994. The radio 1400-MHz and far-infrared (FIR) $60 \mu\text{m}$ luminosities of NGC5996 are 21.8 and 9.9 (in log scale) respectively. These values are consistent with the radio-FIR correlation (Yun, Reddy & Condon 2001).

5.2 H I in M51-type systems

As mentioned earlier, the H I distribution of Arp72 has been found to be very similar to those of M51 and Arp86, categorised as M51-type systems. Although detailed modeling of Arp72 is beyond the scope of this paper, we summarise the similarities in the H I morphology and kinematics in these systems, and discuss the possible kinematic models for such systems (e.g. Toomre & Toomre 1972; Salo & Laurikainen 1993; Theis & Spinnaker 2003).



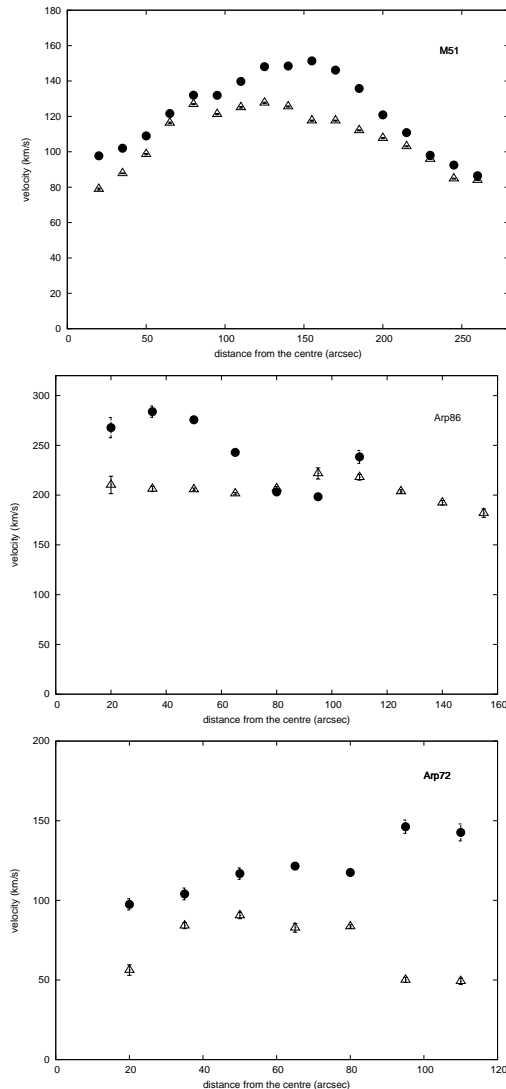


Figure 6. Rotation curves of the approaching and receding sides of the NGC5194 (M51) in the M51 system (upper panel), NGC7753 in the Arp86 system (middle panel) and NGC5996 in the Arp72 system (lower panel). The triangles indicate the receding side and the filled circles indicate the approaching side.

The H I distributions of the M51-type systems we have observed so far, Arp72 and Arp86, have striking similarities with those of M51. In both cases the centres of the main disks show H I depletion, and a prominent H I bridge is seen to connect the two interacting galaxies. The low-resolution images show that from the edges of the main disks of both the systems, a long H I tail originates and just like the M51 system, curves back and runs almost parallel to the bridge between the two galaxies. Like M51 this extension is seen only in lower H I column densities. The H I column density limit for this in all the three cases is $\leq 3 \times 10^{20}$ atoms cm^{-2} . On the opposite side of the disk, towards the companion, in all three cases, a similar but smaller low-density H I extension without any optical counterpart has been seen.

This apparent similarity in their H I morphology may have its origin in the kind of interactions these systems may have gone through. Early test particle simulations by Toomre & Toomre (1972) suggested that the M51 system was experiencing its first close passage encounter. However, to explain the new H I

tidal feature observed by Rots et al. (1990), about 2 to 3 times longer duration of perturbation was necessary than proposed by Toomre & Toomre (1972), suggesting multiple passage encounters (Hernquist 1990). Howard & Byrd (1990) carried out a detailed simulation of the M51 system including disk self gravitation and using a three component (stars, gas clouds, inert halo) model. With a single, recent passage of the companion past an initially unperturbed disk model, they could explain most of the spiral features of the system, but the extended tidal features like the long tail found by Rots et al. (1990) remained unexplained. They concluded that the extended tidal arm seen by Rots et al. (1990) was in fact a remnant of a previous passage of the companion.

M51 is not an isolated case and two of the M51-type systems we have observed, show similar features and would thus require the multiple passage model to explain the observed features. As discussed in Sengupta et al. (2009), we see that the ratio of the masses of the companion NGC5195 to the main galaxy NGC5194 in the case of the M51 system, needed to be roughly 0.1 for the simulation to be able to reproduce the observational features (Howard & Byrd 1990). From the H α rotation curves, the masses of NGC7753 and NGC7752 in the Arp86 system were estimated to be $1.3 \times 10^{11} M_{\odot}$ and $1.8 \times 10^{10} M_{\odot}$ respectively (Marcelin et al. 1987). This makes the mass ratio of the companion to the main galaxy ~ 0.1 , a value similar to that of the M51 system (Howard & Byrd 1990). For the Arp72 system, the K-band mass ratios for the two galaxies were estimated. The estimated mass of NGC5996 and NGC5994 are $2.7 \times 10^{10} M_{\odot}$ and $2.3 \times 10^9 M_{\odot}$ respectively. The companion to main galaxy mass ratio is again ~ 0.1 , similar to those of the Arp86 and M51 systems. Thus the mass ratios being also similar in all three systems, is consistent with their interactions being similar.

The results from the simulations and rotation curve analysis of the Arp86 system by Salo & Laurikainen (1993) suggests an M51-like interaction involving multiple passages of the companion. In our study of Arp86, we suggested that the long northern tidal tail may be a remnant from the past passage of the companion (Sengupta et al. 2009). We notice a similar long tidal arm to the north east of the Arp72 system. Though no simulation results exist for this system, from a comparison of the H I features with those of the other two systems, we suggest that Arp72 has also probably undergone a similar multiple passage encounter with its companion.

5.2.2 H I kinematics

The velocity field and rotation curves in interacting systems are often found to be disturbed and irregular, due to perturbation by the companion galaxy (Rubin & Ford 1983; Chengalur, Salpeter & Terzian 1994; Salo & Laurikainen 2000; Fuentes Carrera et al. 2004). Normally, kinematic disturbances are expected to fade out within a few rotation cycles (≤ 1 Gyr) (Dale et al. 2001). Therefore these anomalies are of importance as they can be used to trace the interaction history of the system (Kronberger et al. 2006). One such noticeable signature of perturbation is when the rotation curve of one side of the disk declines while the other side remains steady, the so called ‘bifurcation’ of the rotation curve. This happens mainly due to the presence of a close companion. Based on such signatures of disturbances, efforts are being made to use them as timers of the stage of interaction and understand the possible orbits of the companion (Pedrosa et al. 2008; Fuentes Carrera et al. 2004).

Salo & Laurikainen (2000) investigated the single and multiple passage scenarios for the M51 system, and found that high velocity particles in the streamers and also evidence of significant

out of plane velocities, support a recent perturbation and hence the multiple passage model of interaction. A comparison of the rotation curves of the single passage and multiple passage encounter simulations showed that in a single passage the curve remains similar to the circular velocity curve and in the multiple passage the curve declines after a certain radius. Although H α images and velocity fields of M51 and Arp86 have been published earlier (Rots et al. 1990; Sengupta et al. 2009), the H α rotation curves for the dominant galaxies of the M51, Arp86 and Arp72 systems are presented for the first time in Fig. 6. The companion galaxies are too small to obtain rotation curves. THINGS data have been used to obtain the rotation curve of NGC5194 (M51), while the rotation curves of NGC7753 (Arp86) and NGC5996 (Arp72) have been derived using the *GMRT* data. The Groningen Image Processing System (GIPSY), has been used to obtain the rotation curves from the FITS files of the velocity fields. The best fit curves for all the three systems have been obtained by keeping the inclination angle and centre coordinates as fixed parameters and rotational velocity and position angle as free parameters in the ‘ROTCUR’ program of GIPSY.

For NGC5194, both the curves show signs of declining velocity towards the edge, the approaching side falling faster than the receding side (Fig. 6, upper panel). The companion is at the tip of the approaching side, about 300 arcsec away. The ‘S’-shaped profile is also seen for the H α rotation curves observed for the M51 system (Tilanus & Allen 1991). A similar trend of declining H α rotation curve is seen on one side of the Arp86 system, where the companion is present. The side nearer to the companion, shows higher rotation velocity and faster decline near $\sim 100''$ from the centre (Fig. 6, middle panel), which is roughly the distance to the companion. The curve on the receding side remains undisturbed and flat till a longer distance of $\sim 160''$. The decline of rotation velocity near $100''$ is in agreement with the results of (Marcelin et al. 1987), where the authors report a falling H α rotation curve for the western side of NGC7753. The rotation curves of NGC5996 of Arp72 are shown in Fig. 6 (lower panel). A declining H α rotation curve for the receding side of NGC5996 is again apparent. The curve shows signs of a rapid decline near a radial distance of $\sim 80''$ from the centre, which is roughly the distance to the companion. It would be interesting to examine the H α rotation curves with data at other wavelengths. Thus for all these systems, we do notice a similar nature of declining rotation curves, especially on the side where the companion is present, suggesting a similarity with the results of Salo & Laurikainen (1993) that a multiple passage model can often explain these systems better than a single passage model as proposed by Toomre & Toomre (1972).

6 CONCLUDING REMARKS

GMRT observations of the interacting galaxies NGC5996 and NGC5994, which make up the Arp72 system show a complex distribution of H α tails and a bridge between the two galaxies due to tidal interactions between them. Optical, infrared and ultraviolet observations all show a bridge between the two galaxies, and a tail on the eastern side, which is seen most clearly in the *GALEX* image at ultraviolet wavelengths. A range of H α column densities from $\sim 1.7\text{--}2 \times 10^{21}$ atoms cm^{-2} to $0.8\text{--}1.8 \times 10^{20}$ atoms cm^{-2} are seen to be associated with sites of star formation in the bridge, disk of the main galaxy and the tidal debris. There is a depletion of H α in the centre of the more massive galaxy, possibly due to the gas being in the molecular phase as well as ionization of the gas by the starburst in the central region of NGC5996. No star forming zone has

been found to be completely free of any H α association or correlated with very low H α column densities. The morphological and kinematic similarities of Arp72 with M51 and Arp86, suggest a multiple passage model of Salo & Laurikainen (1993) is preferred over the single passage model of Toomre & Toomre (1972), to understand the H α features in M51 systems. The striking similarities for the three M51-type systems discussed here suggest similar time-scales. Howard & Byrd (1990) estimate the period of the companion’s orbit to be 500 Myr, and that it merges in less than three orbits. The orbital period for Arp86 is similar to within a factor of ~ 2 (see Salo & Laurikainen 1993). Identification of such systems at high redshifts from sensitive H α surveys using the upcoming telescopes and modelling the kinematics would provide valuable inputs towards estimating the range of time scales of minor mergers and our understanding of galaxy evolution. A detailed study of Arp72 at H α and say, CO, to compare the kinematics of the ionized and molecular gas with the H α gas would provide a more complete picture of the kinematics and star formation of this interesting M51-type system.

7 ACKNOWLEDGMENTS

We thank an anonymous reviewer for his/her comments which helped improve the manuscript, and Beverly Smith for providing us very promptly with the files of the images. We thank the staff of the *GMRT* who have made these observations possible. The *GMRT* is operated by the National Centre for Radio Astrophysics of the Tata Institute of Fundamental Research. This research has made use of the NASA/IPAC Extragalactic Database (NED) which is operated by the Jet Propulsion Laboratory, California Institute of Technology, under contract with the National Aeronautics and Space Administration.

REFERENCES

- Abraham R.G., Tanvir N.R., Santiago B.X., Ellis R.S., Glazebrook K., van den Bergh S., 1996, *MNRAS*, 279, L47
- Baars J. W. M., Genzel R., Pauliny-Toth I. I. K., Witzel A., 1977, *A&A*, 61, 99
- Balzano V.A., 1983, *ApJ*, 268, 602
- Barnes D.G., 2001, 2001, *MNRAS*, 322, 486
- Barnes J.E., 1999, in *Galaxy interactions at low and high redshift*, eds. J.E. Barnes & D.B. Sanders, Dordrecht: Kluwer, p. 137
- Barnes J.E., Hernquist L.E., 1992, *ARA&A*, 30, 705
- Becker R.H., White R.L., Helfand D.J., 1995, *ApJ*, 450, 559
- Bigiel F., Leroy A., Walter F., Brinks E., de Blok W.J.G., Madore B., Thornley M.D., 2008, *AJ*, 136, 2846
- Boselli A., et al., 2005, *ApJ*, 623, L13
- Bruns C., et al., 2005, *A&A*, 432, 45
- Calzetti, D., et al., 2005, *ApJ*, 633, 871
- Calzetti, D., et al., 2007, *ApJ*, 666, 870
- Chengalur J. N., Salpeter E. E., Terzian Y., 1994, *AJ*, 107, 1984
- Collison P.M., Saikia D.J., Pedlar A., Axon D.J., Unger S.W., 1994, *MNRAS*, 268, 203
- Condon J.J., 1992, *ARA&A*, 30, 575
- Condon J.J., Cotton W.D., Broderick J.J., 2002, *AJ*, 124, 675
- Condon J.J., Cotton W.D., Greisen E.W., Yin Q.F., Perley R.A., Taylor G.B., Broderick J.J., 1998, *AJ*, 115, 1693
- Dale D. A., Giovanelli R., Haynes M. P., Hardy E., Campusano L. E., 2001, *AJ*, 121, 1886

- Dressel L., Condon J.J., 1978, *ApJS*, 36, 53
- Fenech D.M., Muxlow T.W.B., Beswick R.J., Pedlar A., Argo M.K., 2008, *MNRAS*, 391, 1384
- Fuentes-Carrera I., et al., 2004, *A&A*, 415, 451
- Giovanardi C., Salpeter E.E., 1985, *ApJS*, 58, 623
- Greve T.R., et al., 2005, *MNRAS*, 359, 1165
- Hancock M., Smith B.J., Struck C., Giroux M.L., Appleton P.N., Charmandaris V., Reach W.T., 2007, *AJ*, 133, 676
- Harris J., 2007, *ApJ*, 658, 345
- Helfer T.T., Thornley M.D., Regan M.W., Wong T., Sheth K., Vogel S.N., Blitz L., Bock, D.C.J., 2003, *ApJS*, 145, 259
- Hernquist L., 1990, in Wielen R., ed., *Dynamics and Interactions of Galaxies*, Springer, Heidelberg, p 108
- Hota A., Saikia D.J., Irwin J.A., 2007, *MNRAS*, 380, 1009
- Howard S., Byrd Gene G., 1990, *AJ*, 99, 1798
- Hummel E., Saikia D.J., 1991, *A&A*, 249, 43
- Kandalyan R.A., 2003, *A&A*, 398, 493
- Kennicutt Robert C., Jr., 1989, *ApJ*, 344, 685
- Kennicutt R.C., Schweizer F., Barnes J.E., *Galaxies: Interactions and induced star formation*, Berlin: Springer
- Klein U., Wielebinski R., Beck R., 1984, *A&A*, 135, 213
- Kojoian G., Tovmasian Kh.M., Dickinson D.F., Dinger A.S.C., 1980, *AJ*, 85, 1462
- Kronberger T., Kapferer W., Schindler S., Bhm A., Kutdemir E., Ziegler B. L., 2006, *A&A*, 458, 69
- Larson R.B., Tinsley B.M., 1978, *ApJ*, 219, 46
- Leroy A.K., Walter F., Brinks E., Bigiel F., de Blok W.J.G., Madore B., Thornley M.D., 2008, *AJ*, 136, 2782
- Leroy A.K., et al., 2009, *AJ*, 137, 4670
- Marcelin M., Lecoarer E., Boulesteix J., Georgelin Y., Monnet G., 1987, *A&A*, 179, 101
- Neff S.G., et al., 2005, *ApJ*, 619, L91
- Nikola T., Geis N., Herrmann F., Madden S.C., Poglitsch A., Stacey G.J., Townes C.H., 2001, *ApJ*, 561, 203
- Pedrosa S., Tissera P. B., Fuentes-Carrera I., Mendes de Oliveira C., 2008, *A&A*, 484, 299
- Reshetnikov V.P., Klimanov S.A., 2003, *AstL*, 29, 429
- Rots A. H., Bosma A., van der Hulst J. M., Athanassoula E., Crane P. C., 1990, *AJ*, 100, 387
- Rubin V. C., Ford W. K. Jr., 1983, *ApJ*, 271, 556
- Ryan R.E. Jr., Cohen S.H., Windhorst R.A., Silk J., 2008, *ApJ*, 678, 751
- Ryan-Weber E.V., et al., 2004, *AJ*, 127, 1431
- Saikia D.J., Unger S.W., Pedlar A., Yates G.J., Axon D.J., Wolsencroft R.D., Taylor K., Gyldenkerne K., 1990, *MNRAS*, 245, 397
- Saikia D.J., Pedlar A., Unger S.W., Axon D.J., 1994, *MNRAS*, 270, 46
- Salo H., Laurikainen E., 1993, *ApJ*, 410, 586
- Salo H., Laurikainen E., 2000, *MNRAS*, 319, 377
- Sanders D.B., Mirabel I.F., 1996, *ARA&A*, 34, 749
- Sanders D.B., Soifer B.T., Elias J.H., Madore B.F., Matthews K., Neugebauer G., Scoville N.Z., 1988, *ApJ*, 325, 74
- Schmidt M., 1959, *ApJ*, 129, 243
- Schwartz C.M., Martin C.L., Chandar R., Leitherer C., Heckman T.M., Oey M.S., 2006, *ApJ*, 646, 858
- Schweizer F., 2000, *RSPTA*, 358, 2063
- Schweizer F., 2005, *ASSL*, 329, 143
- Sengupta C., Dwarakanath K.S., Saikia D.J., 2009, *MNRAS*, 397, 548
- Smith B.J., Kleinmann S.G., Huchra J.P., Low F.J., 1987, *ApJ*, 318, 161
- Smith B.J., Struck C., Hancock M., Appleton P.N., Charmandaris V., Reach W.T., 2007, *AJ*, 133, 791
- Smith B.J., Giroux M.L., Struck C., Hancock M., 2010, *AJ*, 139, 1212
- Soifer B.T., Sanders D.B., Madore B.F., Neugebauer G., Danielson G.E., Elias J.H., Lonsdale C.J., Rice W.L., 1987, *ApJ*, 320, 238
- Struck C., 1999, *Phys. Rep.*, 321, 1
- Struck-Marcell C., Tinsley B.M., 1978, *ApJ*, 221, 562
- Theis C. & Spinneker C., 2003, *Ap&SS*, 284, 495
- Tilanus R.P.J., Allen R.J., 1991, *A&A*, 244, 8
- Toomre A. & Toomre J., 1972, *ApJ*, 178, 623
- Walter F., Brinks E., de Blok W.J.G., Bigiel F., Kennicutt R.C., Thornley M.D., Leroy A., 2008, *AJ*, 136, 2563
- Wong O.I., Webster R.L., Kilborn V.A., Waugh M., Staveley-Smith L., 2009, *MNRAS*, 399, 2264
- Woods D.F., Geller M.J., Barton E.J., 2006, *AJ*, 132, 197
- Yun M. S., Reddy N. A., Condon J. J., 2001, *ApJ*, 554, 803